Adsorption and Reactions of Acetaldehyde on Pt(S)-[6(111)×(100)]

Robert W. McCabe,* Craig L. DiMaggio,

Physical Chemistry Department, General Motors Research Laboratories, Warren, Michigan 48090

and Robert J. Madix

Department of Chemical Engineering, Stanford University, Stanford, California 94305
(Received: August 27, 1984)

Adsorption and reaction of acetaldehyde with clean and oxygen-predosed Pt(S)-[6(111)×(100)] were studied by electron energy loss vibrational spectroscopy (EELS) and temperature-programmed reaction spectroscopy (TPRS). Acetaldehyde adsorption at 95 K on the clean surface produced a multilayer structure with vibrational bands characteristic of solid acetaldehyde. This condensed phase desorbed near 133 K leaving an adsorbed layer showing a major binding state of 58 kJ g-mol^{-1} and a minor state of 70 kJ g-mol^{-1}. The vibrational spectra and characteristic pattern of H_2 evolution obtained upon heating the chemisorbed layer above 300 K indicated the conversion of the acetaldehyde surface complex to η^3-ethylidyne. The ethylidyne species dehydrogenated to gaseous hydrogen and surface carbon above 450 K. In a separate reaction path, acetaldehyde underwent decarbonylation near 290 K to produce adsorbed CO and methane, which desorbed in a reaction-limited peak at 317 K. Vibrational features suggestive of a surface acetyl species were observed below 290 K. Evidence was also obtained for acetaldehyde adsorbed molecularly in η^2 configurations. Similar results were obtained for acetaldehyde on the Pt-(S)-[6(111)×(100)] surface in the presence of preadsorbed atomic oxygen, indicating the absence of direct attack of acetaldehyde by oxygen. This contrasts with the nucleophilic attack on the carbonyl carbon observed previously on copper and silver surfaces.

Introduction

Acetaldehyde is of concern as a pollutant in the exhaust from vehicles operated on pure ethanol fuel.[1-3] Studies have been initiated to determine the feasibility of controlling emissions of acetaldehyde from ethanol-fueled vehicles by the use of exhaust catalytic converters containing supported noble-metal or transition-metal oxide catalysts.[4-6] Catalysts are desired that promote the oxidation of acetaldehyde to CO_2 and H_2O at low catalyst temperatures (<400 K) because acetaldehyde emissions are greatest during warmup of the engine and catalytic converter.

Pt supported on alumina at a loading of 0.1 wt % is more active for the oxidation of acetaldehyde to CO_2 and water than alumina-supported transition-metal oxide catalysts containing 4 wt % Cu–2 wt % Cr or 4 wt % Mn.[4] The present study was undertaken to characterize adsorption and reaction of acetaldehyde on single-crystal platinum for the purpose of understanding the basis for the high oxidation activity of platinum relative to the transition-metal oxide catalysts. In addition, we are interested in comparing adsorption and reaction behavior of acetaldehyde on single-crystal platinum with acetaldehyde chemistry in transition-metal complexes.

We are not aware of previous studies of acetaldehyde adsorption or reaction on Pt single-crystal surfaces. The adsorption of acetaldehyde on polycrystalline Pd was studied by Luth et al. with ultraviolet photoelectron spectroscopy (UPS).[7] Decomposition of acetaldehyde occurred at room temperature as evidenced by the photoemission spectrum which was characteristic of molecular CO. Adsorption of acetaldehyde at 120 K on Pd, however, resulted in only a small amount of decomposition to CO. The adsorption and oxidation of acetaldehyde on Cu(110) were studied by Bowker and Madix using temperature-programmed reaction spectroscopy (TPRS).[8] Acetaldehyde was chemisorbed weakly on the clean Cu(110) surface and desorbed without reacting with the surface at ~220 K. In the presence of a quarter monolayer of preadsorbed atomic oxygen, acetaldehyde adsorbed more strongly (T_p increased by ~20 K) and a portion of the acetaldehyde reacted directly with the surface oxygen atoms to form an adsorbed acetate species which decomposed near 590 K. CO_2 and CH_4 were the principal gases produced during decomposition of acetate on Cu(110).

In the present study, high-resolution electron energy loss spectroscopy (EELS) was used in tandem with temperature-programmed reaction spectroscopy (TPRS) to identify surface reaction intermediates and gaseous products of the reactions of acetaldehyde with clean and oxygen-predosed Pt(S)-[6(111)×(100)]. The Pt(S)-[6(111)×(100)] surface was chosen to provide surface sites of different metal atom coordination. Results of these experiments performed under ultrahigh-vacuum conditions are compared with experiments on Cu(110)[8] to obtain qualitative insight into differences between acetaldehyde oxidation on group 10 and group 11 catalysts.

Experimental Section

Experiments were performed in an ion-pumped ultrahigh-vacuum chamber equipped with a LEED system, single-pass cylindrical mirror analyzer Auger electron spectrometer, quadrupole mass spectrometer, and low-energy electron energy loss spectrometer. The apparatus and electron energy loss spectrometer have been described in detail previously.[9]

The Pt crystal was cut and polished on both sides to within 0.5° of the Pt(S)-[6(111)×(100)] orientation. The crystal was then spot-welded to tantalum heating leads and mounted on a liquid-nitrogen-cooled sample manipulator. The crystal was heated resistively, and the temperature could be held constant at values between 95 and 1300 K or ramped linearly from 95 to ~1000 K with a feedback temperature controller. The crystal was cleaned by a combination of argon ion bombardment (front face only) followed by annealing and heating in oxygen at 1225 K. This procedure resulted in a Pt crystal with no impurities detectable by Auger spectroscopy. Acetaldehyde (reagent grade) was further purified by drying over Union Carbide 4A molecular sieve and distilling. The purity was checked by gas-phase IR spectroscopy at a pressure of 25 torr as well as by mass spectrometry in the ultrahigh-vacuum chamber.

Acetaldehyde was dosed onto the front face of the crystal held at 95 K with a multichannel array doser. Multilayer coverages

(1) Gunby, P. *J. Am. Med. Assoc.* **1980**, *243*, 1967.
(2) Bailey, W. H.; Edwards, C. F., paper presented as part of the Proceedings of the 4th International Symposium on Alcohol Fuels Technology, Guaruja, Sao Paulo, Brazil, Oct 1980.
(3) Goodrich, R. S. *Chem. Eng. Prog.* **1982**, *78*, 29.
(4) McCabe, R. W.; Mitchell, P. J. *Ind. Eng. Chem. Prod. Res. Dev.* **1983**, *22*, 212.
(5) McCabe, R. W.; Mitchell, P. J. *Ind. Eng. Chem. Prod. Res. Dev.* **1984**, *23*, 196.
(6) Yao, Y.-F. *Ind. Eng. Chem. Process Des. Dev.* **1984**, *23*, 60.
(7) Luth, H.; Rubloff, G. W.; Grobman, W. D. *Surf. Sci.* **1977**, *63*, 325.
(8) Bowker, M.; Madix, R. J. *Appl. Surf. Sci.* **1981**, *8*, 299.
(9) Sexton, B. A. *J. Vac. Sci. Technol.* **1979**, *16*, 1033.

0022-3654/85/2089-0854$01.50/0

TABLE I: Vibrational Frequencies (cm^{-1}) and Assignments of Acetaldehyde-d_0 and -d_4 Condensed on Pt(S)-[6(111)×(100)] at 95 K[a]

	CH_3CHO			CD_3CDO		
assignt[b]	approx description[b]	crystalline CH_3CHO[b]	CH_3CHO on Pt(S)-[6(111)×(100)]	approx description[b]	crystalline CD_3CDO[b]	CD_3CDO on Pt(S)-[6(111)×(100)]
$\nu_1(A')$	$\nu_{as}(CH_3)$	3003 (m)	2990	$\nu_{as}(CD_3)$	2255 (m)	2240
$\nu_2(A')$	$\nu_s(CH_3)$	2918 (m)	2920 (sh)	$\nu_s(CD_3)$	2133 (s)	2120
$\nu_3(A')$	$\nu(CH)$	2747 (s)	2745 (sh?)	$\nu(CD)$	2095 (s)	2080 (sh?)
$\nu_4(A')$	$\nu(CO)$	1722 (vs)	1720 1650 (sh) chemisorbed	$\nu(CO)$	1712 (vs)	1705 1640 (sh) chemisorbed
$\nu_5(A')$	$\delta_{as}(CH_3)$	1422 (s)	1430	$\nu(CC); \delta_s(CD_3)$	1158 (s)	1165
$\nu_{12}(A'')$	$\delta(CH_3)$	1431 (s)		$\delta(CD_3)$	1040 (m)	1020
$\nu_6(A')$	$\delta(CH)$	1389 (m)	1360	$\delta_{as}(CD_3)$	1014 (s)	
$\nu_7(A')$	$\delta_s(CH_3); \nu(CH)$	1347 (s)		$\delta(CD); \delta_s(CD_3)$	n.o.	n.o.
$\nu_8(A')$	$\gamma_r(CH_3); \nu(CC)$	1118 (s)	1120	$\delta_s(CD_3); \gamma_r(CD_3)$	936 (m)	940–950
$\nu_{13}(A'')$	$\gamma(CH); \gamma_r(CH_3)$	1102 (m)	n.r.	$\gamma(CD); \gamma_r(CD_3)$	948 (m)	
$\nu_9(A')$	$\nu(CC); \gamma_r(CH_3)$	882 (m)	n.o.	$\nu(CC); \gamma_r(CD_3)$	n.o.	n.o.
$\nu_{14}(A'')$	$\gamma(CH); \gamma_r(CH_3)$	770 (m)	n.o.	$\gamma_r(CD_3); \gamma(CD)$	567 (vw)	n.o.
$\nu_{10}(A')$	$\delta(CCO)$	519 (s)	540	$\delta(CCO); \gamma_r(CD_3)$	445 (s)	450

[a] Abbreviations: n.o. = not observed, n.r. = not resolved; vs = very strong, s = strong, m = moderate, w = weak, vw = very weak, sh = shoulder. [b] Reference 10.

of acetaldehyde were formed without the background pressure exceeding 1×10^{-9} torr (1 torr = 133 Pa). Normal background pressure during the course of the experiments with acetaldehyde was $\sim 5 \times 10^{-10}$ torr. Some experiments were made with acetaldehyde-d_4 (99% deuterium) which was obtained from Merck and used without additional purification after its cleanliness was confirmed by gas-phase IR and mass spectrometry. Oxygen (99.99%) was admitted through a conventional leak valve and checked for contamination with the mass spectrometer.

Experiments were performed by first dosing the clean or oxygen-predosed Pt crystal with acetaldehyde at 95 K to form a multilayer coverage. Electron energy loss spectra were then taken at 95 K and after warming the crystal briefly to successively higher temperatures and cooling to 95 K in between to record spectra. Care was taken to ensure that species did not adsorb from background during the course of an annealing experiment. Energy loss spectra obtained after heating the crystal directly to a given temperature and cooling to 95 K were identical with spectra obtained after stepwise heating and cooling at intermediate temperatures prior to reaching the given temperature.

Temperature-programmed reaction (TPR) experiments were carried out by heating the crystal containing a multilayer coverage of acetaldehyde from 95 K at a linear rate of 13 K s^{-1} while recording the multiplexed mass spectrum of desorbed species. Some TPRS experiments with acetaldehyde-d_4 were carried out by heating from 95 to 773 K in a single sweep with the crystal in line of sight of the mass spectrometer ionizer. All of the TPRS data for acetaldehyde-d_0 and the remainder of the acetaldehyde-d_4 data were obtained during interrupted heating sequences associated with the EELS annealing experiments where the crystal was positioned inside the energy loss analyzer.

Results

Vibrational Spectrum of Multilayer Acetaldehyde. Figure 1 (95 K spectrum) shows the vibrational energy loss spectrum of acetaldehyde after dosing at a crystal temperature of 95 K. The vibrational bands are listed in Table I, and assignments are made by comparison with the normal-coordinate analysis of acetaldehyde by Hollenstein and Gunthard based on their detailed study of the solid-state and gas infrared spectra of isotopic species of acetaldehyde.[10] Table I also shows energy loss features for acetaldehyde-d_4 adsorbed at 95 K on the Pt crystal. With the exception of the band appearing as a shoulder at 1650 cm^{-1} for acetaldehyde-d_0 (1640 cm^{-1} for acetaldehyde-d_4), all of the vibrational features correspond closely in frequency to vibrational modes reported by Hollenstein and Gunthard for crystalline films of acetaldehyde-d_0 and -d_4. The normal-coordinate and force field

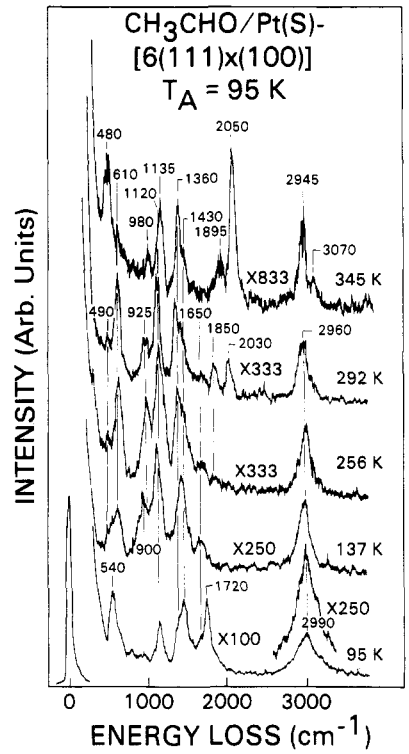

Figure 1. EELS annealing sequence for a 6-L dose of CH_3CHO adsorbed at 95 K on the Pt(S)-[6(111)×(100)] surface. Spectra were recorded at 95 K after heating the surface briefly to the temperatures indicated. Spectra were measured in the specular direction with a primary beam energy near 2 eV.

analyses of Hollenstein and Gunthard indicate that the vibrational modes of acetaldehyde are highly coupled and that most modes consist of several group coordinates.[10] The vibrational modes in Table I have been described only by their major components.

The front face of the Pt crystal was dosed with ~6 L (1 L = 10^{-6} torr s) of acetaldehyde in forming the surface layer shown in the 95 K energy loss spectrum of Figure 1. We estimate from the relative areas of desorption peaks for multilayer and chemisorbed acetaldehyde in subsequent TPRS experiments that acetaldehyde coverages corresponding to 2–3 monolayer equivalents were produced by the 6-L dose. Since thick layers of condensed acetaldehyde were not formed at the relatively low doses employed in this study, the 95 K spectrum of Figure 1 may show vibrational features associated with the chemisorbed layer in addition to the condensed phase. In particular, the band which occurs as a shoulder near 1650 cm^{-1} on the low-frequency side of the carbonyl stretching band does not correspond to any absorption band re-

(10) Hollenstein, H.; Gunthard, Hs. H. *Spectrochim. Acta* **1971**, *27A*, 2027.

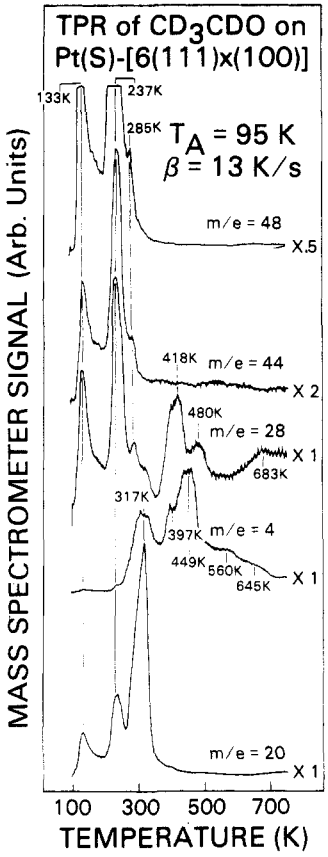

Figure 2. TPR spectra of a multilayer coverage of CD_3CDO adsorbed at 95 K on Pt(S)-[6(111)×(100)]. The heating rate was 13 K s^{-1}. The m/e 48 spectrum was cut off by saturation of the analog-to-digital converter used to acquire the multiplexed mass spectrometer data.

ported for gaseous or solid acetaldehyde.[10] We associate the band at 1650 cm^{-1} (1640 cm^{-1} for acetaldehyde-d_4) with the carbonyl stretching mode of a *chemisorbed* species and attribute the downshifted frequency relative to gas-phase or solid acetaldehyde to bonding interactions with the Pt surface which will be discussed below.

TPRS of Acetaldehyde on Pt(S)-[6(111)×(100)]. Figure 2 shows a set of multiplexed TPR spectra obtained after dosing the crystal at 95 K with 6 L of acetaldehyde-d_4. Spectra are shown for m/e 48 (acetaldehyde-d_4), 44 (CO_2 and a cracking fragment of acetaldehyde-d_4), 28 (CO and a cracking fragment of acetaldehyde-d_4), 20 (D_2O and CD_4), and 4 (D_2). The parent ion spectrum (m/e 48) was cut off at a signal of 10 V where the analog-to-digital converter used to acquire the computer-multiplexed TPR data was saturated. However, the shape and peak temperatures of the parent ion spectrum are reflected in the m/e 44 and 28 spectra, both of which contain cracking fragments of acetaldehyde-d_4. The m/e 44 and 28 spectra show peaks for multilayer acetaldehyde near 133 K and chemisorbed acetaldehyde near 237 K. In addition, the desorption peak near 237 K has a small shoulder near 285 K. The m/e 48 spectrum of Figure 2 shows that complete desorption of acetaldehyde occurs by ~325 K. Figure 2 also shows the D_2 (m/e 4) spectrum from TPR of acetaldehyde-d_4 on Pt(S)-[6(111)×(100)]. The peak at 317 K is within the normal temperature range for the coverage-dependent desorption of H_2 (or D_2) from Pt(111).[11] This indicates that acetaldehyde reacts with the surface to produce hydrogen atoms at temperatures below 317 K. Most of the D_2 desorbed at higher temperatures in a broad band containing multiple peaks. Collins and Spicer observed hydrogen desorption near 420 K from step sites on Pt(S)-[6(111)×(100)].[12] A poorly resolved shoulder appears near 397 K in the D_2 spectrum of Figure 2 which is attributed to desorption of D_2 from step sites. Most of the D_2 desorbed above the normal desorption temperatures associated with either terrace or step sites on Pt(S)-[6(111)×(100)]. The high-temperature region of the D_2 TPR trace in Figure 2 is similar to TPR data reported by Steininger et al.[13] and by Creighton and White[14] for hydrogen evolved during the decomposition of an adsorbed ethylidyne species on Pt(111). Analysis of the surface by AES after TPR to 773 K showed residual carbon at a C(273 eV)/Pt(238 eV) peak height ratio of ~0.4. Creighton and White, using static secondary ion mass spectrometry, observed carbon residue after ethylidyne decomposition on Pt(111).[14]

The m/e 20 spectrum in Figure 2 contains contributions due to CD_4 and/or D_2O. The peaks at 133 and 237 K occur concomitantly with desorption of multilayer and chemisorbed acetaldehyde-d_4 and are associated with methane and/or water produced by mass spectrometer fragmentation and reaction of acetaldehyde-d_4 at surfaces other than the Pt crystal. The peak at 317 K, however, clearly results from a surface reaction as methane and water both desorb at temperatures well below 317 K on Pt surfaces.[15] Corresponding results with acetaldehyde-d_0 showed a m/e 16 peak at 317 K but no m/e 18 peak. These experiments establish methane as a product, but water cannot be ruled out, as readsorption of water onto surfaces in the spectrometer may have prevented its detection.

The m/e 28 spectrum of Figure 2 shows low-temperature features associated with fragmentation products of acetaldehyde-d_4. However, additional peaks associated with adsorbed CO are observed at temperatures near 418 and 480 K. The 418 K peak closely matches the desorption temperature of CO adsorbed at terrace sites on Pt(S)-[6(111)×(100)].[12] The 480 K peak occurs about 60 K lower than normal CO desorption from step sites on Pt(S)-[6(111)×(100)][12] and suggests the presence of coadsorbed "contaminant" species along the steps. Carbon-containing residues, such as the ethylidyne species evidenced by the characteristic shape of the high-temperature D_2 desorption spectrum, may play this role.

CO also desorbs over the temperature range of 600–850 K where the reaction of adsorbed carbon with adsorbed oxygen atoms is known to result in CO desorption from Pt single-crystal surfaces.[16] However, the amount of CO which desorbed in the 600–850 K range varied widely between experiments and may have resulted from warming of the sample holder at the high crystal temperatures.

The m/e 44 spectrum was obtained to check for the formation of CO_2 by surface reactions of acetaldehyde. As noted above, the peaks at 133 and 237 K (shoulder at 285 K) are associated with fragmentation of acetaldehyde-d_4. No CO_2 desorption was observed.

Vibrational Analysis of Acetaldehyde Layers after Heating. Figures 1 and 3 show vibrational spectra for acetaldehyde-d_0 and -d_4, respectively, after dosing at 95 K and heating to successively higher temperatures (the surface was recooled to 95 K to record spectra). The principal changes in the vibrational spectrum of acetaldehyde-d_0 after heating to 137 K to desorb the multilayer were (1) disappearance of the carbonyl stretching mode at 1720 cm^{-1} resulting in clear resolution of a weak absorption band at ~1650 cm^{-1}, (2) appearance of a new band near 900 cm^{-1}, and (3) a loss of intensity in the region of the skeletal bending mode (500–550 cm^{-1}) and appearance of a new band at 610 cm^{-1}. Similar changes were observed in the vibrational spectrum of acetaldehyde-d_4 (Figure 3) after heating to 154 K: (1) disappearance of the carbonyl stretching mode at 1720 cm^{-1} leaving a weak mode at ~1650 cm^{-1} and (2) loss of intensity in the region of the skeletal bending mode (ca. 450 cm^{-1}) together with the appearance of a weak, poorly resolved feature near 545 cm^{-1}. The presence of the $\delta_s(CD_3)$ mode near 950 cm^{-1} precludes analysis of the 154 K spectrum for the development of a new band near

(11) Christmann, K.; Ertl, G.; Pignet, T. *Surf. Sci.* **1976**, *54*, 365. McCabe, R. W.; Schmidt, L. D. *Surf. Sci.* **1977**, *65*, 189.
(12) Collins, D. M.; Spicer, W. E. *Surf. Sci.* **1977**, *69*, 85.
(13) Steininger, H.; Ibach, H.; Lehwald, S. *Surf. Sci.* **1982**, *117*, 685.
(14) Creighton, J. R.; White, J. M. *Surf. Sci.* **1983**, *129*, 327.
(15) Fisher, G. B.; Gland, J. L. *Surf. Sci.* **1980**, *94*, 446.
(16) Netzer, F. P.; Willie, R. A. *J. Catal.* **1978**, *51*, 18.

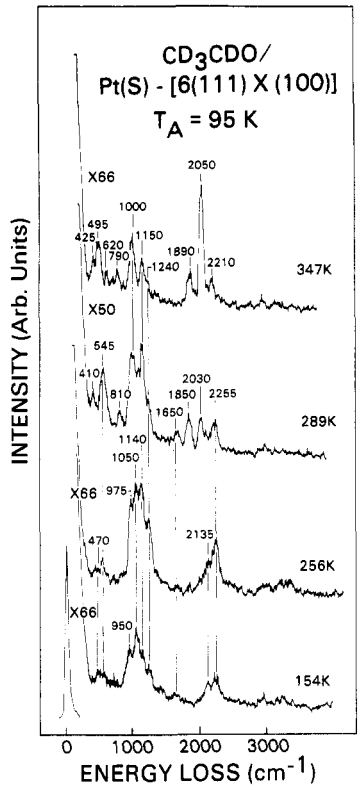

Figure 3. EELS annealing sequence for a 6-L dose of CD_3CDO adsorbed at 95 K on Pt(S)-[6(111)×(100)]. Spectra were obtained in the same manner as Figure 1.

900 cm^{-1} analogous to the new band observed in the spectrum of acetaldehyde-d_0 after heating to 137 K. No band emerged between 545 and 950 cm^{-1}.

The new vibrational features observed after heating both acetaldehyde-d_0 and -d_4 above 133 K are due to either chemisorption-induced shifts in band frequencies of acetaldehyde or formation of a new surface species. With regard to the latter possibility, the dissociative chemisorption of acetaldehyde as a platinum acetyl species and atomic hydrogen appears likely in view of the ease with which platinum acyl complexes are formed.[17] We note, however, that vibrational modes associated with the aldehydic hydrogen were not clearly resolved in the spectra of either the condensed or chemisorbed phases; hence, EELS data do not provide direct evidence for this conversion.

The adsorbed layer was next heated briefly to 256 K to desorb acetaldehyde at 237 K. No new vibrational bands appeared after heating to 256 K, and the overall intensities of the acetaldehyde-d_0 and -d_4 spectra were not greatly affected by the loss of this state. These observations suggest that more than one adsorbed species is present at low temperatures with the predominant species (i.e., that desorbing at 237 K) having weak vibrational features. Only subtle changes occurred in the vibrational spectra as the acetaldehyde-d_0 and -d_4 layers were heated to 256 K; bands near 900 cm^{-1} (acetaldehyde-d_0) and 950 cm^{-1} (acetaldehyde-d_4) shifted upward by about 25 cm^{-1}, and relative band intensities changed in the region of the hydrogen deformation modes. The latter is clearly evident in Figure 4 which shows the hydrogen deformation band region for CD_3CDO and CH_3CHO after heating briefly to temperatures slightly below (dashed curves) and slightly above (solid curves) the main acetaldehyde desorption peak at 237 K. For both acetaldehyde-d_0 and -d_4, there was an intensity decrease in the region of the out-of-plane $\nu_{12}(A'')$ methyl hydrogen deformation mode (1040 cm^{-1} for CD_3CDO and 1430 cm^{-1} for CH_3CHO) *relative* to the intensities of the neighboring in-plane A′ modes. The $\nu_{12}(A'')$ mode is the only "strong" A″ mode of acetaldehyde reported in ref 10 (see Table I) and is the only A″

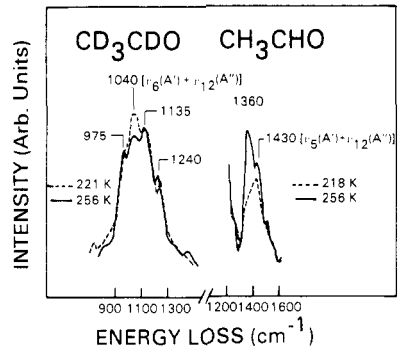

Figure 4. Vibrational spectra of the region of hydrogen deformation modes for (a) acetaldehyde-d_4 and (b) acetaldehyde-d_0 after heating to temperatures just below (- - -) and just above (—) the main acetaldehyde desorption peak at 237 K. Note the changes in *relative* intensities of the bands containing the $\nu_{12}(A'')$ mode compared to neighboring bands. The absolute intensity remained nearly constant for acetaldehyde-d_4 and increased for acetaldehyde-d_0 upon desorption of the 237 K state.

mode clearly detected in this study. Selective loss of intensity in the $\nu_{12}(A'')$ mode relative to the neighboring A′ modes is consistent with the desorption of a flat-lying acetaldehyde species. As will be discussed later, the major vibrational features observed between 133 and 256 K are believed to be associated with acetaldehyde dissociatively adsorbed as an acetyl species and atomic hydrogen.

The spectra of Figure 3 for acetaldehyde-d_4 show a loss at 1240 cm^{-1}. The 1240-cm^{-1} band was evident in the chemisorbed layer formed by heating to 154 K and disappeared after annealing above 270 K. The 1240-cm^{-1} band lies above the frequency range of $\delta(CD_3)$ modes. No corresponding band was observed in the spectra of acetaldehyde-d_0, possibly due to major bands at 1120 and 1360–1420 cm^{-1}. Continued heating to ~290 K resulted in the development of vibrational bands near 1850 and 2030 cm^{-1} for both acetaldehyde-d_0 (Figure 1) and acetaldehyde-d_4 (Figure 3). These bands are associated with bridging and linear carbon monoxide and indicate the onset of carbon–carbon bond cleavage in the chemisorbed acetaldehyde (or acetyl species). The frequency of the bridged CO is identical with that reported for Pt(111)[18] and slightly lower than that reported for Pt(321) (1865 cm^{-1}).[19] The frequency of the linear CO is lower than the value of 2065 cm^{-1} reported for low coverages of CO on both Pt(111)[20] and Pt(321).[19] Coadsorbed species may be responsible for the low stretching frequency of the linear CO.

Heating the surface from 292 to 345 K (Figure 1) resulted in further growth of the bands associated with both bridged and linear CO and shifts to higher frequencies. Concomitantly, the intensities of the bands near 610 and 925 cm^{-1} decreased markedly and the band at 1650 cm^{-1} disappeared. Similar changes were observed in the energy loss spectra of the acetaldehyde-d_4 species (Figure 3) after heating to 347 K. In particular, the bands at ~545 and ~1650 cm^{-1} disappeared. Slight shifts to higher frequency (10–20 cm^{-1}) were observed for the bands near 1120 cm^{-1} in acetaldehyde-d_0 and 1140 cm^{-1} in the acetaldehyde-d_4 spectrum upon heating between 290 and 345 K. The resulting spectra, for both acetaldehyde-d_0 and -d_4 after heating to ~345 K, show close similarity to those reported by Steininger et al.[13] for a surface ethylidyne species formed in the room-temperature decomposition of ethylene on Pt(111).

Oxygen Adsorption on Pt(S)-[6(111)×(100)]. The adsorption of oxygen on the Pt(S)-[6(111)×(100)] surface was briefly examined before carrying out experiments involving coadsorbed acetaldehyde and oxygen. Oxygen adsorption at 95 K was predominantly molecular and was characterized by a strong vibrational loss at 880 cm^{-1} which has been associated with the ν(0–0) stretching mode of a peroxo-type species on Pt(111)[21] and Pt-

(17) Dent, S. P.; Eaborn, C.; Pidcock, A.; Ratcliff, B. *Organomet. Chem.* **1972**, *46*, C68.

(18) Steininger, H.; Lehwald, S.; Ibach, H. *Surf. Sci.* **1982**, *123*, 264.
(19) McClellan, M. R.; Gland, J. L.; McFeeley, F. R. *Surf. Sci.* **1981**, *112*, 63.
(20) Shigeishi, R. A.; King, D. A. *Surf. Sci.* **1976**, *58*, 379.
(21) Gland, J. L.; Sexton, B. A.; Fisher, G. B. *Surf. Sci.* **1980**, *95*, 587.

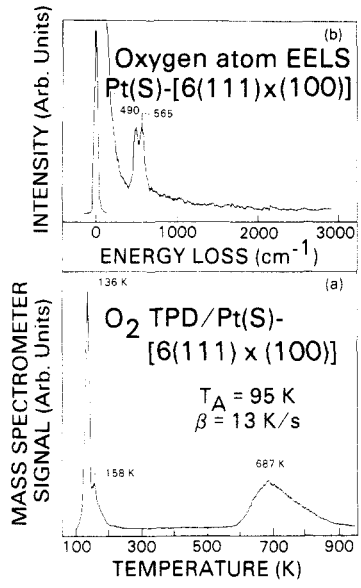

Figure 5. (a) O_2 thermal desorption spectrum for oxygen adsorbed at 95 K on Pt(S)-[6(111)×(100)] showing peaks at 136 and 158 K associated with molecularly adsorbed oxygen and a peak at 687 K associated with atomically adsorbed oxygen. (b) EELS spectrum for oxygen atoms on Pt(S)-[6(111)×(100)]. O_2 was adsorbed at 95 K and dissociated by heating to 373 K.

(321).[22] Figure 5 shows the oxygen temperature-programmed desorption (TPD) spectrum obtained after a 60-L dose of oxygen at 95 K. A narrow peak is observed at 136 K which, by comparison with TPD spectra for oxygen on Pt(111),[21] is associated with desorption of molecular oxygen from terrace sites. A shoulder is observed at 158 K on the main desorption peak for molecular oxygen which is similar to a feature observed by McClellan et al.[22] for molecular oxygen desorption from Pt(321) and which we associate with desorption of molecular oxygen from the step sites on Pt(S)-[6(111)×(100)]. Figure 5 also shows a broad desorption peak characterized by a maximum desorption rate near 690 K. The high-temperature desorption state occurs in the temperature range reported by Gland et al.[21] and by McClellan et al.[22] for desorption of atomically adsorbed oxygen as O_2, from Pt(111) and Pt(321), respectively.

For the purpose of examining the decomposition of acetaldehyde in the presence of adsorbed oxygen, oxygen was first adsorbed at 95 K on the clean Pt(S)-[6(111)×(100)] surface and then heated to 373 K to dissociate molecular oxygen—thereby producing an atomic oxygen overlayer. LEED analysis of the atomic oxygen overlayer showed well-developed half-order spots characteristic of the (2 × 2) LEED pattern associated with a saturation quarter-monolayer coverage of atomic oxygen on Pt(111). EELS provided evidence for adsorption of atomic oxygen at step sites as well as at the terrace sites. Figure 5b shows the energy loss spectrum of the atomic oxygen layer. Two peaks were observed—a peak at 490 cm^{-1} corresponding closely in frequency to the Pt–O stretching mode of atomic oxygen on Pt(111)[21] and a second peak at 565 cm^{-1} corresponding closely with a peak observed by McClellan et al.[22] for atomic oxygen adsorbed at step sites on Pt(321). Thus, our starting surface for the study of acetaldehyde decomposition in the presence of oxygen contained oxygen atoms adsorbed at both terrace and step sites. We designate this surface Pt(S)-[6(111)×(100)]–O.

Adsorption and Reactions of Acetaldehyde on Pt(S)-[6(111)×(100)]–O. Adsorption of acetaldehyde on the Pt(S)-[6(111)×(100)]–O surface at 95 K resulted in an energy loss spectrum identical with that of the 95 K spectrum for acetaldehyde condensed on the clean surface. The bands at 490 and 565 cm^{-1} associated with atomic oxygen were not observed once the multilayer coverage of acetaldehyde was formed. Figure 6 shows energy loss spectra obtained after heating the layer of condensed

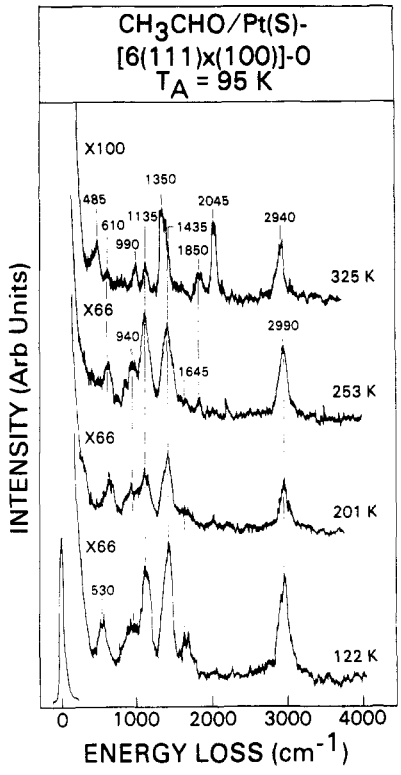

Figure 6. EELS annealing sequence for CH_3CHO on Pt(S)-[6(111)×(100)] with preadsorbed atomic oxygen. Spectra were obtained in the same manner as Figure 1.

acetaldehyde on the oxygen-predosed surface to successively higher temperatures. The spectra show close similarity to those obtained for acetaldehyde on the clean surface after similar thermal treatment (Figure 1). In particular, the spectra of Figure 6 after heating to 201 and 253 K show features identical with those observed in the clean surface spectra—viz. new bands near 1645, 940, and 610 cm^{-1}. At temperatures above 253 K in Figure 6, bands associated with CO (1850 and 2045 cm^{-1}) appeared and vibrational features characteristic of ethylidyne were observed, also in agreement with results obtained on the clean surface. No new bands were observed during the annealing sequence for acetaldehyde on oxygen-predosed Pt(S)-[6(111)×(100)]. In particular, the energy loss spectra showed no evidence for bands associated with either OH or H_2O. Vibrational bands characteristic of both OH and H_2O on Pt(111) have been identified by Fisher and Sexton.[23] However, the spectra recorded after heating to 122 and 201 K in Figure 6, as well as spectra obtained after heating to intermediate temperatures, showed no evidence for O–H stretching modes (3420 cm^{-1} for H_2O and 3480 cm^{-1} for OH on Pt(111)) or the strong ν(Pt–O) (430 cm^{-1}) and δ(O–H) (1015 cm^{-1}) modes associated with OH on Pt(111); nor were the analogous modes for D_2O or OD observed. H_2O librations on Pt(111) produce an intense, broad band centered near 700 cm^{-1} which also was not observed.

The absence of vibrational features associated with OH or H_2O indicates that direct transfer of hydrogen to oxygen does not occur; i.e., there is no evidence for C–H bond cleavage promoted by hydrogen bonding between acetaldehyde and adsorbed oxygen atoms. Thus, the situation is unlike the reaction between water and oxygen atoms on Pt(111),[23] where direct transfer of hydrogen to oxygen is evidenced by the appearance of vibrational bands associated with OH. In contrast, the reaction of hydrogen atoms with oxygen atoms on Pt(111)[24] has been shown to proceed without the development of spectroscopic features associated with OH species. Thus, any water which is formed from acetaldehyde on Pt(S)-[6(111)×(100)] appears to result from reactions between

(22) McClellan, M. R.; McFeeley, F. R. *Surf. Sci.* **1983**, *124*, 188.

(23) Fisher, G. B.; Sexton, B. A. *Phys. Rev. Lett.* **1980**, *44*, 683.

(24) Fisher, G. B.; Gland, J. L.; Schmieg, S. J. *J. Vac. Sci. Technol.* **1982**, *20*, 518.

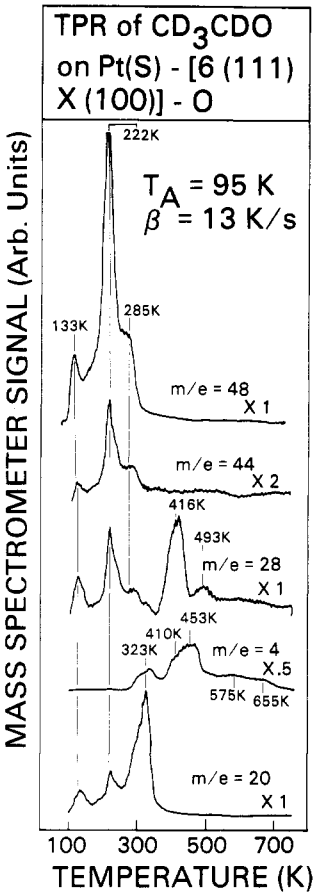

Figure 7. TPR spectra of a multilayer coverage of CD_3CDO on Pt(S)-[6(111)×(100)] with preadsorbed atomic oxygen.

adsorbed hydrogen atoms and oxygen atoms.

The absence of vibrational features characteristic of the OH functional group in the acetaldehyde spectra on both the clean and oxygen-predosed surfaces also indicates that acetaldehyde does not adsorb or react via the enol configuration. Furthermore, the vibrational doublet near 1000 cm^{-1}, characteristic of CH_3C-HOO,[25] was not observed. Thus, adsorbed oxygen does not act as a strong nucleophile as it does on silver.[26] Figure 7 shows a set of multiplexed TPR spectra for acetaldehyde-d_4 adsorbed at 95 K on the Pt(S)-[6(111)×(100)]-O surface. The starting surface contained only slightly more than monolayer coverage of acetaldehyde-d_4 as evidenced by the relatively low peak area of the desorption state for condensed acetaldehyde-d_4 near 133 K relative to the peak area for the main chemisorbed state at 222 K. Otherwise, the TPR spectra are quite similar to those observed for acetaldehyde-d_4 on the clean surface (Figure 2) except for (1) small temperature shifts in some peaks—most notably the main acetaldehyde peak which shifts downward by ~15° to 222 K—and (2) changes in relative intensities of some peaks. We note the absence of significant desorption of mass 44 above 300 K, indicating that CO_2 is not formed during acetaldehyde decomposition either by decomposition of acetate as is observed for acetaldehyde on oxygen-covered Cu(110)[8] or by secondary reactions between CO and atomic oxygen. These results suggest that oxygen is removed from the surface as H_2O at temperatures near 317 K or below.

The *m/e* 28 TPR spectrum in Figure 7 is qualitatively similar to its counterpart for acetaldehyde-d_4 on the clean surface. The peaks at 416 and 493 K are associated with CO desorbed from terrace and step sites, respectively. More desorption of terrace and step site CO was observed relative to hydrogen-containing species (CH_4 and H_2) on the oxygen-predosed surface (Figure 7) than on the clean surface (Figure 2). To illustrate, the CO(416 K)/CD_4(323 K) peak height ratio for the oxygen-predosed surface is 0.8 in Figure 7, whereas the corresponding CO(418 K)/CD_4(317 K) peak height ratio for the clean surface is 0.45 in Figure 2. Similarly, the CO(416 K)/D_2(323 K) peak height ratio for the oxygen predosed surface is 2.2 in Figure 7, whereas the corresponding CO(418 K)/D_2(317 K) peak height ratio for the clean surface is 1.4 in Figure 2. These results further support our assumption that some of the hydrogen which contributes to H_2 and CH_4 production on the clean surface instead reacts with O(a) to form H_2O on the oxygen-predosed surface. We also note that less desorption of CO occurs at temperatures above 600 K in Figure 7 than in the corresponding clean surface CO TPR trace (Figure 2). However, as we noted previously, the amount of high-temperature CO varied considerably from experiment to experiment.

The *m/e* 4 spectrum for D_2 in Figure 7 shows evidence for normal D_2 desorption from terrace and step sites on Pt(S)[6-(111)×(100)] as well as features characteristic of ethylidyne decomposition. In addition, residual carbon was also observed on the oxygen-predosed surface after TPR to 773 K, however, at a slightly lower concentration (Auger C(273 eV)/Pt(238 eV) = 0.32) than on the clean surface (Auger C(273 eV)/Pt(238 eV) = 0.39).

The *m/e* 20 spectrum of Figure 7 shows close agreement with the *m/e* 20 spectrum of Figure 2 for the clean surface. As for the clean surface, the low-temperature peaks at 133 and 222 K occur simultaneously with peaks for multilayer and chemisorbed acetaldehyde and are associated with cracking fragments of acetaldehyde. The peak near 323 K is attributed to CD_4 generated by surface reactions of acetaldehyde-d_4 which are initiated near 290 K. In addition, the 323 K peak may contain a small contribution due to D_2O generated during the decomposition of acetaldehyde-d_4.

Discussion

Decomposition Pathways of Acetaldehyde on Pt(S)-[6(111)×(100)]. Acetaldehyde reacted with both the clean and oxygen-predosed surfaces by two pathways: (1) *simultaneous* formation of CO(a) and CH_4 and (2) formation of adsorbed ethylidyne. Pathway 1 requires cleavage of the acetaldehyde C–C bond and reaction of the aldehydic hydrogen at the methyl group, either via intramolecular transfer, i.e.

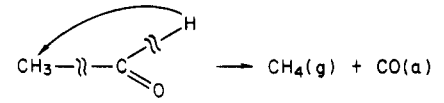

or via transfer to the surface and subsequent reaction with surface methyl species. An acetyl intermediate must be formed if the C–H bond breaks first; otherwise, the formyl intermediate must be formed. Several mechanisms are possible for pathway 2 leading to ethylidyne: (2a) C—C bond cleavage in acetaldehyde or acetyl with subsequent reactions between surface CH_x (x = 0–3) species and (2b) C=O bond cleavage (leading directly to ethylidyne in the case of an acetyl precursor or requiring subsequent loss of the aldehydic hydrogen for the acetaldehyde precursor). We are not aware of examples of mechanism 2a in ultrahigh-vacuum studies. Benziger and Madix[27] examined the reactions of CH_3 groups produced by decomposition of CH_3Cl on Fe(100) and found methane and elemental carbon to be the only products; there was no evidence for hydrocarbon fragments with carbon number greater than one. Similarly, CH_4 has been observed as a product in other studies of alcohol[28,29] and aldehyde[29] reactions with transition-metal surfaces, but no hydrocarbon products greater than C_1 have been reported. A C_2H_x species has been observed in acetone decomposition at accidental step sites on Pt(111);[30] however, for acetone, intramolecular reactions as well as mechanism 2a could produce the C_2H_x species.

(25) Stuve, E. M.; Madix, R. J. *Surf. Sci.* **1982**, *119*, 279.
(26) Barteau, M. A.; Bowker, M.; Madix, R. J. *Surf. Sci.* **1980**, *94*, 303.
(27) Benziger, J. B.; Madix, R. J. *J. Catal.* **1982**, *74*, 55.
(28) Ko, E. I.; Madix, R. J. *Surf. Sci.* **1981**, *112*, 373.
(29) Johnson, S. W.; Madix, R. J. *Surf. Sci.* **1982**, *115*, 61.
(30) Avery, N. R. *Surf. Sci.* **1983**, *125*, 771.

TABLE II: Comparison of Vibrational Frequencies (cm^{-1}) of Adsorbed Acetaldehyde-d_0 and -d_4 with Vibrational Frequencies of (a) a Platinum Acetyl Complex (Ref 31) and (b) an Acetaldehyde-Solvated Ni Complex (Ref 32)[a]

(a) Comparison with *trans*-$[PtBr(CO{\cdot}CX_3)(PEt_3)_2]$ (X = H or D)

	trans-$[PtBr(CO{\cdot}CX_3)(PEt_3)_2]$ in CCl_4 solution			CX_3CXO on Pt(S)-[6(111)×(100)] after heating to 132–137 K		
acetyl mode	X = H	X = D	ν_H/ν_D	X = H	X = D	ν_H/ν_D
ν(MC)	537 (m)	470 (w)	1.14	~490 (sh)	~470 (sh)	1.04
δ(CCO)	584 (m)	522 (w)	1.12	610	545	1.12
ν(CC)	909 (m)	838 (w)	1.09	900–925	n.r.	
$\gamma(CH_3)$	1080 (vs)	967 (s)	1.12	1120	975	1.15
ν(CO)	1630 (vs)	1639 (vs)	0.99	1650	1650–1670	1.00–0.99

(b) Comparison with $Ni(CH_3CHO)_6(FeCl_4)_2$

acetaldehyde mode[b]	acetaldehyde gas[b]	$Ni(CH_3CHO)_6(FeCl_4)_2$	CH_3CHO on Pt(S)-[6(111)×(100)] after heating to 137 K
ν(MO)		282	n.o.
δ(CCO)	509	568	610
ν(CC); $\gamma_r(CH_3)$	867	n.o.	900–925
$\gamma_r(CH_3)$; ν(CC)	1118	1130	1120
ν(CO)	1743	1665	1650

[a] Abbreviations: n.o. = not observed, n.r. = not resolved. [b] Reference 6.

Vibrational Evidence for Acetyl Intermediate. Similarities between the vibrational spectra of platinum acetyl complexes and acetaldehyde chemisorbed on the Pt crystal provide evidence for acetaldehyde decomposition via abstraction of the aldehydic hydrogen, producing an acetyl intermediate and an H adatom. Table II compares species present after heating only enough to remove the multilayer (137 K) with (I) a platinum acetyl complex, *trans*-$[PtBr(CO{\cdot}CX_3)(PEt_3)_2]$ (X = H or D), where the acetyl group is bonded to Pt by the carbonyl carbon,[31] and (II) an acetaldehyde-solvated nickel complex, $Ni(CH_3CHO)_6(FeCl_4)_2$, in which the acetaldehyde molecules form weak donor bonds to the Ni atom through their oxygen atom.[32] The band at 610 cm^{-1} in the energy loss spectra correlates more closely with the δ(CCO) mode of (I) (584 cm^{-1}) than with the δ(CCO) mode in either solid acetaldehyde (519 cm^{-1})[10] or (II) (568 cm^{-1}). Thus, we associate the band at 610 cm^{-1} with the δ(CCO) mode of a surface acetyl species and attribute the weak shoulder feature at 490 cm^{-1} (470 cm^{-1} for acetaldehyde-d_4) with the ν(PtC) stretch of the acetyl species. Additional evidence for the acetyl species is obtained by analyzing the region of the ν(CC); $\gamma_r(CH_3)$ mode which occurs at 882 cm^{-1} in solid acetaldehyde (Table I). The band is not observed in the spectrum of condensed acetaldehyde; i.e., no energy loss features above the noise level are apparent in the 95 K spectrum of Figure 1. Similarly, the band was not reported for (II) (Table IIB). Absence of the ν(CC); $\gamma_r(CH_3)$ mode is not surprising, however, considering that it is weak in the gas phase and of medium intensity in the solid phase.[10] With the exception of the $\nu(CH_3)$ modes, only those modes of solid acetaldehyde identified as "strong" in ref 10 were observed in the spectrum of condensed acetaldehyde. Further, we are not aware of other EELS studies where vibrational bands are absent in condensed-phase spectra, yet become visible in the chemisorbed layer. The reverse is generally observed—random orientation of molecules in the condensed phase leads to EELS activity of all modes, but some modes are absent in the chemisorbed layer due to dipole selection rules. These considerations lead to the conclusion that the band at 900–925 cm^{-1} in the chemisorbed layer is not a mode of acetaldehyde. Instead the new mode occurs at the same frequency as the ν(CC) mode in (I), thereby providing further support for a surface acetyl intermediate in acetaldehyde decomposition on Pt. The acetyl features in the vibrational spectra persist, without loss of intensity up to ~290 K, and are in no way correlated with the 237 and 285 K desorption peaks.

Bonding Configurations of Chemisorbed Acetaldehyde. The absence of A′ modes associated with acetaldehyde desorbing in the 237 K state, together with the reduced intensity of the ν_{12}(A″) out-of-plane hydrogen deformation mode (Figure 4) after desorption of the 237 K peak, indicates that acetaldehyde bonds molecularly in the 237 K state with its skeletal plane parallel to the surface. Moreover, the 15° decrease in peak temperature for the 237 K state in the presence of preadsorbed atomic oxygen suggests an acceptor-type bond since adsorbed oxygen will withdraw charge from Pt, thereby reducing the extent of back-bonding and weakening the bond to the surface. As is evident from Figure 8, showing the 3A″ π^*_{CO} antibonding orbital of acetaldehyde (the lowest unfilled molecular orbital), an acceptor bond can be formed between the 3A″ orbital and the Pt d_{xz} orbitals, either through (1) the carbon and oxygen atoms (Figure 8a) in a configuration analogous to that proposed for back-donation in π-bonded olefin complexes or (2) the oxygen atom only (Figure 8b) in a configuration analogous to the back-bonding to the π^*_{CO} lobes centered on the carbon atom in CO. Given the angles of emergence of the Pt d_{xz} orbitals (30° relative to the surface plane for the (111) orientation and 45° for the (100) orientation in the related t_{2g} ligand field orbitals[34]), we propose the η^2 configuration (Figure 8a) since the flat-lying orientation is consistent with the vibrational data. Similar π-bonding configurations have previously been reported for a hexafluoroacetone nickel complex[35] and for acetone adsorbed at accidental step sites on Pt(111).[30]

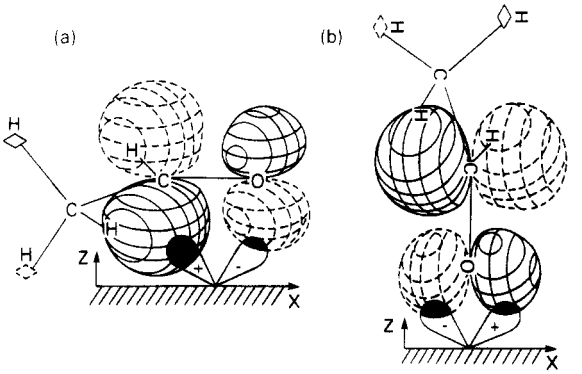

Figure 8. Schematic diagrams of possible acceptor-type bonds between acetaldehyde and the $Pt_{d_{xz}}$ orbitals. The 3A″ π^*_{CO} antibonding orbital of acetaldehyde is shown (as reproduced from ref 33). Bonding in (a) is analogous to back-donation in olefin complexes, while that in (b) is analogous to back-donation to carbon in CO. Configuration (a) is proposed for acetaldehyde in the 237 K state since the acetaldehyde molecular plane will be nearly parallel to the surface, as suggested by the vibrational data.

(31) Adams, D. M.; Booth, G. *J. Chem. Soc.* **1962**, 1112.
(32) Driessen, W. L.; Groeneveld, W. L. *Recl. Trav. Chim. Pays-Bas* **1971**, *90*, 87.
(33) Jorgensen, W. L.; Salem, L. "The Organic Chemist's Book of Orbitals"; Academic Press: New York, 1973; p 142.
(34) Bond, G. C. *Discuss. Faraday Soc.* **1966**, *41*, 200.
(35) Countryman, R.; Penfold, B. R. *J. Cryst. Mol. Struct.* **1972**, *2*, 281.

Finally, the spectra indicate the possibility of a minority di-σ-bonded species leading to the small vibrational loss at 1240 cm^{-1} most clearly seen in the d_4 spectra. Di-σ-bonding has been observed in hexafluoroacetone complexes[36,37] and in a Ta(η^5-C_5Me_5)(η^2-$(CH_3)_2CO$)Me_2 complex (Me = CH_3)[38] where the carbonyl stretching frequency occurs near 1200 cm^{-1}, and has also been proposed for acetone adsorbed on Ru(001) where a band is observed at 1280 cm^{-1}.[39] The 1240-cm^{-1} band persisted to temperatures above 270 K and, therefore, cannot be associated with the π-bonded species giving rise to the major desorption peak at 237 K, but instead may be associated with the 285 K state.

Comparison of Acetaldehyde Reactions on Pt and Cu. Comparison of these results with data obtained by Bowker and Madix for acetaldehyde adsorption and reaction on Cu(110) reveals significant differences between Pt and Cu as catalysts for the reactions of acetaldehyde.[8] The most striking difference between metals is the effect of chemisorbed oxygen on the reactions of acetaldehyde. Acetaldehyde does not react on Cu(110) in the absence of chemisorbed oxygen but forms acetate in the presence of chemisorbed oxygen. The Pt(S)-[6(111)×(100)] crystal, on the other hand, showed no evidence for direct reaction of acetaldehyde with oxygen atoms. Similar conclusions were reached by Sexton et al.[40] in a study of ethanol reactions with clean and oxygen-predosed Pt(111)—oxygen did not react directly with ethanol but only served to remove, as H_2O, the hydrogen that was produced during ethanol decomposition. Thus, decomposition reactions predominate on the Pt crystal surface while direct oxidation of acetaldehyde (i.e., oxygen addition) occurs on Cu(110). With regard to the tendency toward decomposition reactions on Pt, we note that the evidence obtained in this study for acetaldehyde decomposition to CO and CH_4 via an acetyl intermediate parallels the mechanism of the homogeneously catalyzed decarbonylation of acetaldehyde.[41,42] The high activity which has been observed for acetaldehyde oxidation over alumina-supported Pt relative to an alumina-supported copper-containing catalyst[4] appears to be consistent with reaction mechanisms indicated from the surface chemistry studies on Pt and Cu. The acetate species that formed during oxidation of acetaldehyde on Cu(110)[8] was quite stable (decomposition occurred near 590 K). In contrast, this study shows that the acetyl intermediate decomposes near 290 K on Pt(S)-[6(111)×(100)]. Thus, the rate-limiting step in acetaldehyde oxidation on Cu catalysts may be decomposition of a strongly adsorbed acetate intermediate while on Pt catalysts the oxidation of decomposition products, such as CO, hydrogen, and hydrocarbon residues, may be rate limiting.

Conclusions

The following observations have been made:

1. Multilayer acetaldehyde desorbs with an activation energy of 32 kJ $g\text{-}mol^{-1}$ leaving a chemisorbed phase characterized by acetaldehyde desorption states with desorption activation energies of 58 kJ $g\text{-}mol^{-1}$ (major state) and 70 kJ $g\text{-}mol^{-1}$ (minor state).

2. Acetaldehyde adsorbs in the major state in a lying-down π-bonded configuration barely visible with EELS. The minor state may be associated with a di-σ-bonded molecular acetaldehyde species. The most prominent vibrational features between 137 and 290 K appear to be those of an acetyl species, identified by similarities to the infrared spectra of Pt acetyl complexes.

3. Acetaldehyde decomposes on Pt(S)-[6(111)×(100)] by the scheme outlined below which summarizes the major reactions involving carbon-containing species. Reactions 2–4 parallel the mechanism of homogeneous acetaldehyde decarbonylation. In (5), we cannot distinguish between possible mechanisms for ethylidyne formation involving either carbon–carbon or carbon–oxygen bond dissociation.

$$CH_3CHO(g) \underset{237\ K}{\rightleftharpoons} CH_3CHO(a) \quad (1)$$

$$CH_3CHO(a) \xrightarrow{<137\ K} CH_3CO(a) + H(a) \quad (2)$$

$$CH_3CO(a) \xrightarrow{\sim 290\ K} CH_3(a) + CO(a) \quad (3)$$

$$CH_3(a) + H(a) \xrightarrow{317\ K} CH_4(g) \quad (4)$$

$$\left.\begin{array}{l} CH_3CO(a) \xrightarrow{\sim 290\ K} C_2H_3(a) + O(a) \\ \text{or} \\ 2CH_3CO(a) \xrightarrow{\sim 290\ K} C_2H_3(a) + 2CO(a) + 3H(a) \end{array}\right\} \quad (5)$$

$$C_2H_3(a) \xrightarrow{450\ K} 2C(a) + {}^3/_2H_2(g) \quad (6)$$

$$CO(a) \xrightarrow{418\ K} CO(g) \quad (7)$$

4. Reaction pathways are identical for acetaldehyde on the clean surface and the surface with preadsorbed atomic oxygen, indicating that acetaldehyde does not react directly with preadsorbed atomic oxygen under ultrahigh-vacuum conditions, unlike the group 11 metals Cu and Ag.

(36) Clarke, B.; Green, M.; Osborn, R. B. L.; Stone, F. G. A. *J. Chem. Soc. A* **1969**, 20.
(37) Green, M.; Howard, J. A. K.; Laguna, A.; Smart, L. E.; Spencer, J. L.; Stone, F. G. A. *J. Chem. Soc., Dalton Trans.* **1977**, 278.
(38) Wood, C. D.; Schrock, R. R. *J. Am. Chem. Soc.* **1979**, *101*, 5421.
(39) Avery, N. R.; Weinberg, W. H.; Anton, A. B.; Toby, B. H. *Phys. Rev. Lett.* **1983**, *51*, 682.
(40) Sexton, B. A.; Rendulic, K. D.; Hughes, A. E. *Surf. Sci.* **1982**, *121*, 181.
(41) Sheldon, R. A.; Kochi, J. K. "Metal-Catalyzed Oxidations of Organic Compounds"; Academic Press: New York, 1981; pp 359–361.
(42) Milstein, D. *Acc. Chem. Res.* **1984**, *17*, 221.